Journal of Engineering Science and Technology
Vol. 10, No. 5 (2015) 633 - 653

MECHANISTIC KINETIC MODELS FOR STEAM REFORMING OF CONCENTRATED CRUDE ETHANOL ON NI/AL_2O_3 CATALYST

O. A. OLAFADEHAN[1,*], A. A. AYOOLA[2], O. O. AKINTUNDE[1], V. O. ADENIYI[1]

[1]Department of Chemical Engineering, University of Lagos, Akoka-Yaba, Lagos State, Nigeria
[2]Department of Chemical Engineering, Covenant University, Canaan Land, Ota, Ogun State, Nigeria
*Corresponding Author: oolafadehan@unilag.edu.ng

Abstract

Mechanistic kinetic models were postulated for the catalytic steam reforming of concentrated crude ethanol on a Ni-based commercial catalyst at atmosphere pressure in the temperature range of 673-863 K, and at different catalyst weight to the crude ethanol molar flow rate ratio (in the range 0.9645-9.6451 kg catalyst h/kg mole crude ethanol) in a stainless steel packed bed tubular microreactor. The models were based on Langmuir-Hinshelwood-Hougen-Watson (LHHW) and Eley-Rideal (ER) mechanisms. The optimization routine of Nelder-Mead simplex algorithm was used to estimate the inherent kinetic parameters in the proposed models. The selection of the best kinetic model amongst the rival kinetic models was based on physicochemical, statistical and thermodynamic scrutinies. The rate determining step for the steam reforming of concentrated crude ethanol on Ni/Al_2O_3 catalyst was found to be surface reaction between chemisorbed CH_3O and O when hydrogen and oxygen were adsorbed as monomolecular species on the catalyst surface. Excellent agreement was obtained between the experimental rate of reaction and conversion of crude ethanol, and the simulated results, with ADD% being ±0.46.

Keywords: Crude ethanol, Steam reforming, Mechanism, Kinetic model, Optimization, Rate-determining step.

1. Introduction

The combustion of non-renewable energy resources, such as fossil fuels, constitutes the supply of the majority of current energy needs. However, this is associated with the release of large quantities of greenhouse gases (GHG), especially carbon dioxide (CO_2), nitrogen oxides (NO_x), hydrocarbons and other

Nomenclatures

AAD	Average absolute deviation
B	Oxygenated hydrocarbon fraction, CH_2O
C	Carbon dioxide
C_i	Bulk concentration of component i, kmol/m^3
C_p^0	Heat capacities of component i in the ideal-gas state, J/K
E	Ethanol
E_b	Backward activation energy, J/mol
E_f	Forward activation energy, J/mol
h	Heat transfer coefficient, J/(m^2 s K)
I	Methane (hydrocarbon)
K_i	Thermodynamic equilibrium adsorption coefficient
k_c	Mass transfer coefficient, m/s
k_i, k_j	Specific reaction rate coefficient
M	Methyl (CH_3)
MO	Methoxide
N	Number of experimental data points
N_{Eo}	Initial molar feed rate of crude ethanol, mol/h
N_i	Molar rate of component *i*, mol/h
N_{Wo}	Initial molar feed rate of steam, mol/h
n	Order of reaction
p	Number of parameters
R	Radius of catalyst particle, m
R_g	Universal gas constant, J/(mol K)
$R_{i,\,cal}$	Calculated rate of component *i*, g mol/(g cat h)
$R_{i,\,obs}$	Observed rate of component *i*, g mol/(g cat h)
S_c	Schmidt number, dimensionless
S_C^2	Combined population variance
S_d (=SD)	Standard deviation of the difference of the means
T	Reaction temperature, K
v	Velocity, m
W	Weight of catalyst, g
X_E	Fractional conversion of crude ethanol, dimensionless
$X_{E,calc}$	Calculated conversion of crude ethanol, dimensionless
$\overline{X}_{E,calc}$	Calculated mean conversion of crude ethanol, dimensionless
$X_{E,obs}$	Observed fractional conversion of crude ethanol, dimensionless
$\overline{X}_{i,obs}$	Observed mean conversion of crude ethanol, dimensionless

Greek Symbols

ΔG	Gibbs free energy, J/mol
$\Delta G^{\circ}_{f,298K}$	Standard Gibbs energy of formation at 298.15 K, J/mol
ΔH_{ads}	Enthalpy of adsorption, J/mol
$\Delta H^{\circ}_{f,298K}$	Standard heats of formation at 298 K, J/mol
ΔH_R	Heat of reaction, J/mol
ΔS_{ads}	Entropy of adsorption, J/mol K

ρ_b	Bulk density of catalyst bed, kg/m^3

Abbreviations

Ipd	Internal pore diffusion
WP	Weisz-Prater

harmful emissions such as particulate matters to the indoor and outdoor atmosphere [1-3]. The gradual depletion of the fossil fuels reserves and efforts to combat pollution and greenhouse gas emissions have stimulated a considerable interest in using alternative resources of energy [4, 5]. Consequently, efforts are being geared toward commercialization of the use of fuel cells such as the proton exchange membrane (PEM) fuel cell. This commercialization can be used for the generation of electric power for both electric vehicles and distributed electric power plants [6] owing to the high-energy efficiency of the fuel cell with an overall energy efficiency of about 85% [7]. With an equally strong interest in the use of hydrogen as the fuel, PEM fuel cells are the most certain to meet future ultra low NO_x, SO_x, CO, CH_4 and CO_2 emission targets [6]. The fast development of fuel cell technologies and particularly of the solid polymer fuel cell (SPFC) [8] involves the storage of a liquid fuel free from sulphur, which is crucial for processes involving metal-based catalysts, and which will be transformable into hydrogen without polluting emissions. Thus, hydrogen (H_2) has a significant future potential as an alternative fuel that can solve the problems of CO_2 emissions as well as the emissions of other air contaminants.

There exists several routes for commercial production of hydrogen on a large scale which include electrolysis of water using Hoffman's apparatus, coal gasification, as off-gases from petroleum refinery operations, steam reforming of natural gas and other fossil fuels [9, 10], autothermal reforming (O_2 is added to equilibrate the endothermicity of the steam reforming reaction) and biomass [11]. Its current worldwide production is about 5×10^{17} m^3 per year [12]. It is primarily used as a feedstock in the chemical industry, for instance, in the manufacture of ammonia and methanol, and in the refinery re-processing and conversion processes. However, a new eco-friendly reservoir of hydrogen is needed if a global cycle of clean and sustainable production of energy is envisaged. A promising route for hydrogen production involves the steam reforming of alcohols, primarily methanol and ethanol. Ethanol, a form of biomass, presents several advantages related to natural availability, storage, handling and safety [13, 14]. Ethanol can be produced renewably from several biomass sources, including energy plants, waste materials from agro-industries or forestry residue materials, organic fraction of municipal solid waste, etc. It ought to be noted that about 352 liters of ethanol can be produced from approximately 1 tonne or 1 acre of wheat. As such, ethanol provides an environmentally responsible energy source that can significantly reduce GHG emissions [5]. The process of bio-ethanol conversion to hydrogen has the significant advantage of being nearly CO_2 neutral [15], since the CO_2 produced is consumed for biomass growth thus offering a nearly closed carbon loop. Furthermore, since ethanol does not contain heteroatoms (such as nitrogen and sulphur which can form different oxides in the presence of oxygen) and metals, its use as source of energy does not result in emissions of NO_x, SO_x, particulate matters and other toxic chemicals.

In addition, ethanol is mostly an oxygenated hydrocarbon, which leads to complete combustion during its application to produce power. As such, little or no CO is produced. Thus, ethanol is economically, environmentally and strategically attractive as an energy source. Ethanol can be a hydrogen source for countries that lack fossil fuel resources, but have significant agricultural economy. This is feasible because virtually any biomass can now be converted into ethanol as a result of recent advances in biotechnology [16]. These attributes have made H_2 obtained from ethanol reforming a very good energy vector, especially in fuel cells applications. Hydrogen production from ethanol has advantages compared to other H_2 production techniques, including steam reforming of methanol and hydrocarbons. Unlike hydrocarbons, ethanol is easier to reform and is also free of sulphur, which is a catalyst poison in the reforming of hydrocarbons [15]. Also, unlike methanol, which is produced from hydrocarbons and has a relatively high toxicity, ethanol is completely biomass-based and has low toxicity and as such it provides less risk to the population [8]. The fact that methanol is derived from fossil fuel resources also renders it an unreliable energy source in the long run. Conclusively, amongst the various processes and primary fuels that have been proposed for hydrogen production in fuel cell applications, steam reforming of ethanol is very attractive. Ethanol reforming, proceeds at temperatures in the range of 300-600^{o}C, which is significantly lower than those required for CH_4 or gasoline reforming. This is an important consideration for the improved heat integration of fuel cell vehicles. Thermodynamic studies revealed that steam reforming of ethanol is feasible at temperatures higher than 500 K resulting in production of methane, carbon oxides and hydrogen as the main products [17-20].

The production of hydrogen by catalytic steam reforming of pure ethanol has been widely investigated, with different water to ethanol molar ratios [5, 17-20, 21-29]. In all these cases, water was needed as a co-feed to the process. Hence, there is no need to reduce the water and organic contents of fermentation product (fermentation broth produced from a fermentation process) since this contains approximately 12%v/v ethanol, which is within the range of water to ethanol molar ratios used in the literature [21-24]. Besides, by using crude ethanol, the other organic compounds present in the fermentation broth could equally be reformed to produce additional hydrogen. Moreover, this process eliminates the large amount of energy wasted during distillation to remove water from fermentation broth in order to produce dry or pure ethanol. Haga et al. [5] suggested that in order to obtain a widespread use of ethanol for hydrogen production, the economics and energy consumption of the ethanol production process have to be greatly improved. Thus, by circumventing the distillation and drying step, this process of reforming crude ethanol (obtained from fermentation broth) provides an ability to produce hydrogen from crude ethanol solution in a cost-effective manner.

Extensive studies on hydrogen production from ethanol have been reported in the literature [5, 13, 15, 22, 23, 25, 27, 30-34]. However, there is very little or no exhaustive kinetic investigation on the steam reforming of crude ethanol in the literature. Few reports are available in the literature on the mechanism of steam reforming of ethanol [16, 35-44]. Akande [16] and Akande et al. [43] investigated the mechanism of crude ethanol (15% v/v). They formulated their elementary steps using Eley-Rideal (ER) mechanism and reported that the rate determining step is the dissociation of adsorbed ethanol. Diagne et al. [37] reported the reaction mechanism on steam reforming of ethanol over Rh-based catalyst. They suggested that the

limiting step for the production of hydrogen from ethanol is the formation of CH_4 via the surface reaction of adsorbed oxametallacycle intermediate. All the investigators mentioned earlier except Akande [16] and Akande et al. [43] agreed that acetaldehyde is the most likely intermediate formed during ethanol decomposition. Although many kinetic models have been developed for steam reforming of ethanol (as cited above), formulation of a feasible and comprehensive mechanistic rate expression for the reaction is sparse in the literature. Moreover, only limited attempts [41, 42] have been made in testing the validity of their rate expressions against experimentally obtained results. Sun et al. [42] and Vaidya and Rodrigues [44] showed that the steam reforming of ethanol is first order with respect to ethanol. Akande et al. [45] formulated an ER based kinetic model for reforming of crude ethanol by assuming the dissociation of adsorbed ethanol as the rate-limiting step. However, this model did not predict excellently the experimental data of steam reforming of crude ethanol. Thus, there is a need to develop a new and reliable kinetic model for the steam reforming of ethanol, which can be used for sizing the reformer and optimization studies.

The objective of this study was to develop a feasible and comprehensive mechanistic kinetic model for steam reforming of concentrated crude ethanol on Ni/Al_2O_3 catalyst based on atomic and molecular adsorption of oxygen and hydrogen using Langmuir-Hinshelwood-Hougen-Watson (LHHW) and Eley-Rideal (ER) approaches. The inherent kinetic parameters in the kinetic models were estimated using Nelder-Mead simplex optimization scheme, and certain criteria were employed with a view to discriminating amongst rival kinetic models and thus obtain the rate-determining step for the reforming reaction.

2. Development of Mechanistic Kinetic Models for Catalytic Steam Reforming of Concentrated Crude Ethanol

In this study, a detailed and feasible reaction mechanism for steam reforming of concentrated crude ethanol on Ni/Al_2O_3 catalysts was developed. A notable difference in the proposed reaction mechanisms was in the assumption of active sites for the adsorbed species. Since oxygen and hydrogen were involved, two modes of oxygen and hydrogen adsorptions were considered: atomic and molecular, together with the assumption that all adsorbed species compete on the catalyst surface.

Catalytic steam reforming of ethanol on Ni based catalyst is a process that produces primarily hydrogen and carbon dioxide, as well as traces of carbon monoxide (about 1-2 mol%). The main reactions that occur on this type of catalyst are:

- Ethanol steam reforming: $C_2H_5OH + 3H_2O \rightarrow 2CO_2 + 6H_2$ (1)
- Ethanol decomposition to methane: $C_2H_5OH \rightarrow CO + H_2 + CH_4$ (2)
- Ethanol dehydration: $C_2H_5OH \rightarrow C_2H_4 + H_2O$ (3)
- Ethanol dehydrogenation: $C_2H_5OH \rightarrow CH_3CHO + H_2$ (4)
- Ethanol decomposition to acetone: $2C_2H_5OH \rightarrow CH_3COCH_3 + CO + 3H_2$ (5)
- Water-gas shift reaction: $CO + H_2O \rightarrow CO_2 + H_2$ (6)

The development of kinetic model requires a good formulation of elementary steps from the feed materials to products. The overall reaction employed for the

development of the kinetic models for the steam reforming of crude ethanol is given by [44, 46]:

$$C_2H_5OH + 3H_2O \rightarrow 2CO_2 + 6H_2 \quad \Delta H_{298\,K} = +174\ \text{kJ/mol} \tag{7}$$

Ethanol was used as the representative material for crude ethanol for simplicity and owing to its much higher concentration compared to other components that are present in the crude ethanol mixture during the experimental investigation of steam reforming of ethanol [43]. Empirical and mechanistic rate models that were proposed to fit the experimental data are outlined below.

Firstly, different empirical, irreversible power law rate models that were based on fixed feed molar flow rate were proposed as follows [47]:

$$\left(-r_E\right) = k_o e^{-E/RT} N_E^n = kN_E^n \tag{8}$$

$$\left(-r_E\right) = k_o e^{-E/RT} N_E^\alpha N_W^\beta = kN_E^\alpha N_W^\beta \tag{9}$$

$$\left(-r_E\right) = k_o e^{-E/RT} N_E^\alpha \left(A + N_H\right)^\gamma = kN_E^\alpha \left(A + N_H\right)^\gamma \tag{10}$$

Secondly, different mechanistic kinetic models were developed based on Langmuir-Hinshelwood-Hougen-Watson (LHHW) and Eley-Rideal (ER) approaches by considering each of the elementary steps in Cases I, II and III as the rate-determining step and applying quasi-steady state approximation to the other elementary reactions in the proposed mechanisms. However, in the construction of plausible Langmuir-Hinshelwood-Hougen-Watson reaction mechanisms for the reaction expressed in Eq. (1), both atomic and molecular hydrogen adsorptions as well as atomic and molecular adsorptions of oxygen were considered (as stated earlier). For the three different cases considered, the total concentration of active sites, C_T's (as the case may be) consists of vacant and adsorbed sites.

Case I: oxygen and hydrogen are adsorbed as atomic species, and the following assumptions were made:

- Adsorption of crude ethanol is rate-controlling.
- Dissociation of adsorbed crude ethanol to form chemisorbed radicals (CH_3O and CH_3) is rate-controlling.
- Molecular adsorption of steam is rate-controlling.
- Surface reaction of adsorbed steam to produce surface chemisorbed oxygen radical and free hydrogen vapour is rate-controlling.
- Surface reaction between chemisorbed CH_3O and O is rate-controlling.
- Surface reaction between chemisorbed CH_3 and O is rate-controlling.
- Desorption of adsorbed carbon dioxide is rate-controlling.
- Molecular arrangement of adsorbed atomic hydrogen is rate-controlling.
- Desorption of adsorbed molecular hydrogen is rate-controlling, we have:

Case II: oxygen and hydrogen are adsorbed as molecular species, and the following assumptions were made:

Adsorption of crude ethanol is rate-controlling.

- 11.Dissociation of adsorbed crude ethanol to form chemisorbed radicals (CH_3O and CH_3) is rate-controlling.

- Molecular adsorption of steam is rate-controlling.
- Surface reaction of adsorbed steam to produce surface chemisorbed O_2 and free hydrogen vapour is rate-controlling.
- Surface reaction between chemisorbed CH_3O and O_2 is rate-controlling.
- Surface reaction between chemisorbed CH_3 and O_2 is rate-controlling.
- Desorption of adsorbed carbon dioxide is rate-controlling.
- Desorption of adsorbed molecular hydrogen is rate-controlling.

Case III: For the Eley-Rideal mechanism, the following assumptions were made to derive the rate expression for steam reforming of ethanol:

- Molecular adsorption of crude ethanol is rate-controlling.
- Dissociation of adsorbed crude ethanol into chemisorbed radicals (CH_2O and CH_4) is rate-controlling.
- Surface reaction of chemisorbed CH_2O with non-adsorbed water vapour is rate-controlling.
- Surface reaction of chemisorbed CH_4 with non-adsorbed water vapour is rate-controlling.
- Desorption of adsorbed carbon dioxide is rate-controlling.

3. Materials and Methods

The experimental data were obtained at atmospheric pressure (total pressure, $p_T = 1$ atm) using a packed bed reactor at reaction temperatures of 673, 763 and 863 K, and W/N_{Ao} of 0.9645 to 9.6451 g cat h/g mol crude ethanol [46]. The crude ethanol used for the experiment by Akpan et al. [46] was analysed by High Performance Liquid Chromatograph (HPLC), and the results are presented in Table 1.

Table 1. Composition of Crude Ethanol Used [46].

Crude ethanol components	Mol %	Mol % on a water free basis
Ethanol	17.86	78.71
Lactic acid	2.90	12.76
Glycerol	1.93	8.51
Maltose	0.0023	0.01
Water	77.31	Not applicable

Based on this result, the molecular formula for the mixture was found to be $C_{2.17}H_{6.14}O_{1.35}$. Thus, the stoichiometric equation for the reforming of concentrated crude ethanol can be written as:

$$C_{2.17}H_{6.14}O_{1.35} + 2.99H_2O \rightleftharpoons 2.17CO_2 + 6.06H_2 \quad (11)$$

The catalyst used in the experimental investigation was a nickel based commercial catalyst obtained from REB Research and Consulting, Ferndale, MI, USA [46]. The Ni/Al_2O_3 catalyst was used because Ni enhances steam reforming

reaction [23]. Ni also ensures C-C bond rupture of ethanol or other oxygenated hydrocarbon components of crude ethanol [25, 26]. Moreover, nickel enhances ethanol gasification, and reduces selectivity of acetaldehyde and acetic acid [27]. The support used was γ-Al_2O_3 because it is cheaply available, and has high surface area and thermal stability [48]. The details of the experimental procedure and results were reported by Akpan et al. [46]. The experiments were conducted in the regime where mass transfer and diffusion did not affect the kinetics of reaction.

The fractional conversion, X_E of crude ethanol was calculated using the expression below:

$$X_E = \frac{kmol\ organics\ in - kmol\ organics\ out}{kmol\ organics\ in} \tag{12}$$

Organics here refer to ethanol + lactic acid + glycerol + maltose.

For reproducibility of the experimental data, all data presented in this work were repeated thrice and the average taken.

The experimental rates, r_i, of reaction (shown in Table 2) were obtained by differentiating the conversion, X_i, versus space time, W/N_{Eo}, data since the continuity equation of the reaction components in a plug flow tubular reactor is given by $r_i = d\hat{N}/dW$, where $\hat{N}$ is the vector of molar flow rates, N_i, defined as $N_E = N_{Eo}(1 - X_E)$ for ethanol (E); $N_W = N_{Eo}(\theta_W - 2.99X_E)$, $\theta_W = N_{Wo}/N_{Eo}$ for steam (W); $N_C = 2.17N_{Eo}X_E$ and $N_H = 6.06N_{Eo}X_E$ are for the reaction products (carbon dioxide (C) and hydrogen (H) respectively). The expressions for N_E, N_W, N_C and N_H were obtained from the stoichiometric Eq. (11). The molar flow rates of the chemically reactive species participating in the steam reforming of concentrated crude ethanol are presented in Table 2, with the experimental rates obtained thus:

$$(-r_E) = -\frac{1}{W}\frac{dN_E}{dt} = \frac{dX_E}{d(W/\dot{N}_{Eo})} = \frac{dX_E}{d\theta}\ [=]\ \text{g mol crude ethanol/(g cat. h)} \tag{13}$$

The value of the overall thermodynamic equilibrium constant, K_{SR}, was calculated using Eq. (14) [49]:

$$-In\,K_{SR} = \frac{\Delta G^0}{RT} = \frac{\Delta G_0^o - \Delta H_0^o}{RT_0} + \frac{\Delta H_0^o}{RT} + \frac{1}{T}\int_{T_0}^{T}\frac{\Delta C_p^o}{R}dT - \int_{T_0}^{T}\frac{\Delta C_p^o}{RT}dT \tag{14}$$

where

$$\int_{T_0}^{T}\frac{\Delta C_p^o}{RT}dT = \Delta a\,In\left(\frac{T}{T_0}\right) + \left[\Delta b\,T_0 + \left(\Delta c\,T_0^2 + \frac{\Delta d}{\tau^2 T_0^2}\right)\left(\frac{\tau+1}{2}\right)\right](\tau - 1), \quad \tau = \frac{T}{T_0} \tag{15}$$

The values of various constants in Eqs. (14) and (15) are presented in next section.

In agreement with the expression given in Eq. (14), the general expression for K_{SR} was found to be:

$$In\,K_{SR} = -\frac{7295.22}{T} + 17.64\,In\,T - 9.75\times10^{-3}T + 1.0003\times10^{-6}T^2 - \frac{118{,}475}{T^2} - 70.338 \tag{16}.$$

The Nelder-Mead modified simplex optimisation routine was used to estimate the reaction rate constants and adsorption equilibrium constant parameters for the steam reforming of ethanol on Ni/Al_2O_3 catalyst. This method is quite robust, effective, and easily implementable on a digital computer. Details of the method with a comprehensive algorithm/information flow chart for flexible polygon search can be found in Yang et al. [50], which was adapted in this work in MATLAB environment. Derivative methods, although more efficient, are not recommended because of the difficulty of performing both analytical and numerical differentiation needed in their algorithm [51-55]. Although evaluation of the derivatives by difference schemes can be substituted for evaluation of the analytical derivatives, the numerical error introduced, particularly in the vicinity of the extremum can impair the use of such substitutions.

A multi-dimensional search procedure was employed, as there were many parameters to be estimated. The specific reaction rate and thermodynamic equilibrium constants were obtained using the scheme discussed earlier to minimise the sum of squares of all errors between experimental and predicted conversions. Hence, for each model, we find $\underline{K} \in R^m$ that minimizes the sum of square of the residuals, that is:

$$\varepsilon = J(\underline{K}) = \sqrt{\sum_{k=1}^{n} \left[X(\underline{K}, \theta_k) - X_{k,observed} \right]^2} \tag{17}$$

$$\varepsilon = J(\underline{K}) = \sqrt{\sum_{k=1}^{n} \left[r(\underline{K}, \theta_k) - r_{k,observed} \right]^2} \tag{18}$$

subject to $K_i > 0$; $i = 1, 2, \ldots..$, m; where $X(\underline{K}, \theta)$ and $r(\underline{K}, \theta)$ are the respective conversion and rate model as a function of $\underline{K} = [K_1, K_2, ..., K_m]^T$, the vector of regression parameters; and θ, the so-called space time, is the independent variable. θ_k is, of course, the value of θ at the k^{th} data point, $X_{k,observed}$ and $r_{k\ observed}$ are the respective observed value of X and r at the k^{th} data point, and ε is the error.

Minimisation of the sum of squares of all errors between experimental and predicted rates was also used [as given in Eq. (18) to verify the values of the estimated parameters, whereby the predicted rates were obtained using Eq. (13). The number of experimental and simulated data points used in Eq. (17) or (18) was 5. The optimization routine employed initial guesses for all constants until it found no other values that produced a smaller error.

The sets $\{K_i\}$of the required constant parameters that minimise the error as given in Eq. (17) or (18) are the required values of the constant parameters. Having estimated the parameters, further discrimination amongst rival models was effected by means of an analysis of residuals, which tests the adequacy of the models. The *t*-test, which tests for the significance of a regression coefficient, was performed using the equation [56]:

$$t = \frac{\left| \overline{X}_{obs} - \overline{X}_{calc} \right|}{S_d},\ S_d = S_C \sqrt{\frac{2}{n}},\ S_C = \sqrt{\frac{\sum_{i=1}^{n} \left(X_{i,calc} - \overline{X}_{i,calc} \right)^2 + \sum_{i=1}^{n} \left(X_{i,obs} - \overline{X}_{i,obs} \right)^2}{2(n-1)}} \tag{19}$$

The significance of the global regression was evaluated by means of an *F*-test, based upon the ratio of the mean regression sum of squares to the mean residual sum of squares [57], given by:

$$F = \frac{\frac{1}{p}\sum_{i=1}^{n} X_{i,calc}^{2}}{\frac{1}{p-n}\sum_{i=1}^{n}\left(X_{i,obs} - X_{i,calc}\right)^{2}} \quad (20)$$

Moreover, all the kinetic models were assessed against the Boudart-Mears-Vannice guidelines [58, 59] in order to test their thermodynamic adequacy. This criterion for endothermic reaction is given by:

$$\Delta S_{ads} < 12.2 - 0.0014\Delta H_{ads} < 10 \quad (21)$$

where

$$In\,K = \frac{-\Delta H}{RT} + \frac{\Delta S}{R} \quad (22)$$

4. Results and Discussion

Simulations and results would be presented and discussed in this section.

4.1. Simulation results

Heat and mass transfer limitations and their respective effects would be discussed here.

4.1.1. Heat and mass transfer limitations

It is well known that intrinsic kinetic data can only be obtained experimentally in the absence of mass and heat transfer resistances. Theoretical criteria were used to determine whether there were any effects of interparticle and intraparticle mass and heat transfer limitations on the rate of steam reforming of crude ethanol on Ni/Al_2O_3 catalysts at the highest temperature of 863 K used for the reforming reaction. This is due to the fact that the severest mass and heat transfer resistances occur at the highest temperature of the reaction; if at all those resistances exist.

4.1.2. Heat transfer effects

The internal pore heat transfer resistance was estimated using the Prater analysis, given by:

$$\Delta T_{\max,\,particle} = \frac{D_{eff}\left(C_{As} - C_{Ac}\right)\left(\Delta H_R\right)}{\lambda_{eff}} \quad (23)$$

where $\Delta T_{max,\,particle}$ is the upper limit to temperature variation between pellet centre and its surface, ΔH_R is the heat of reaction, C_{As} and C_{Ac} are the respective concentrations at the pellet surface and centre (assumed to be the same as bulk concentration and zero respectively, as suggested by Levenspiel [60], D_{eff} represents the effective mass diffusivity ($=D_{AB}\,\varepsilon_b/\tau$) [61], with D_{AB} being the bulk diffusivity of component A (ethanol) in component B (water), which, in turn, is estimated using Brokaw equation [62]. The value for D_{AB} at the maximum temperature of 863 K was found to be 4.73×10^{-5} m^2/s. The void fraction of the

bed, ε_b, defined as the ratio of the volume occupied by the voids to the total volume of the bed, was estimated to be 0.5. The tortuosity factor, τ , was taken as 8 [61]. The effective diffusivity, D_{eff}, was estimated to be 2.9563×10^{-6} m^2/s. The effective thermal conductivity, λ_{eff}, was obtained using the correlation given by Walas [63] for packed bed tubular reactors: λ_{eff}= (5.5 + 0.05Re)λ, where λ, the molecular thermal conductivity, calculated using Wassiljewa correlation [62], was determined to be 8.57×10^{-5} kJ/(m s K). The effective thermal conductivity, λ_{eff}, was found to be 9.3×10^{-3} kJ/(m s K). Using these values obtained in Eq. (23), a value of 0.2 K was obtained for $\Delta T_{max,\,particle}$, which is indicative of the fact that the pellet more or less had a uniform temperature.

The heat transfer limitation across the gas film was determined by:

$$\Delta T_{\max,\,film} = \frac{L\left(-r_{A,obs}\right)\left(-\Delta H_R\right)}{h} \tag{24}$$

where $\Delta T_{max,\,film}$ is the upper limit of temperature difference between the bulk gas and pellet surface; L is the characteristic length, and ($-r_{A,obs}$) represents the observed rate of reaction. The heat transfer coefficient, h, was estimated from the correlation: $J_H=J_D=(h/C_p v\rho)\mathrm{Pr}^{2/3}$, where J_H is the heat transfer J factor, Pr is Prandtl number ($=C_p\mu/\lambda$), C_p and λ represent the heat capacity and thermal conductivity respectively. The J_D factor is given by the following correlations: $J_D=(0.4548/\varepsilon_b)\mathrm{Re}^{-0.4069}$ and $J_D=(k_c/v)\mathrm{Sc}^{2/3}$ [64]; $\mathrm{Sc}=\mu/\rho D_{AB}$, $\mathrm{Re}=\rho v d_p/\mu(1-\varepsilon_b)$, k_c is the mass transfer coefficient obtained to be 0.33 m/s based on the J factor analogy. The heat transfer coefficient, h, was determined to be 0.57 kJ/(m^2 s K). Hence, a value of 0.4 K was obtained for $\Delta T_{max,\,film}$. Both values of $\Delta T_{max,\,particle}$ and $\Delta T_{max,\,film}$ confirm the absence of heat transfer limitations externally and internally, which lend credence to the assumption of isothermal operation conditions during the steam reforming of crude ethanol [60].

Moreover, a more rigorous criterion for determining the onset of heat transfer limitation during the reforming reaction, developed by Mears [65], was also used to ascertain the absence of heat transfer resistance as given by:

$$\frac{\left(r_{obs}\right)\rho_b RE\left(-\Delta H_R\right)}{hT^2 R_g} < 0.15 \tag{25}$$

On substituting the numerical values for the terms on the left side of Eq. (25), a value of 0.02 was obtained, which is less than 0.15. Hence, heat transport limitation effects are negligible.

4.1.3. Mass transfer effects

The internal pore mass transfer resistance was calculated using Weisz-Prater criterion, given by:

$$C_{WP,ipd} = \frac{\left(-r_{A,obs}\right)\rho_p R^2}{D_{eff} C_{AS}} \tag{26}$$

where $C_{WP,ipd}$ is the Wiesz-Prater criterion for internal pore diffusion, ρ_p the pellet density and R the catalyst radius. The estimated value for $C_{WP,ipd}$ was 0.071,

which is much less than 1. Thus, this is indicative that the concentration on the catalyst surface is indistinguishable from the concentration within its pores, that is, no concentration gradient exists within the pellet. This result comes as a consequence of the absence of internal pore diffusion limitations [61].

To determine whether film mass transfer rate has any effect on the rate of reaction, the ratio of observed rate to the rate if film resistance controls was examined. This criterion is given by:

$$\frac{observed\ rate}{rate\ if\ \ film\ resistance\ controls} = \frac{\left(-r_{A,obs}\right)}{C_{Ab}k_c}\frac{d_p}{6} \tag{27}$$

The estimated value for the ratio in Eq. (27) was 2.5×10^{-6}, which indicates that the observed rate is very much less than the limiting film mass transfer rate. Thus, the resistance to film mass transfer certainly should not influence the rate of reaction [60]. Mears' criterion [61] is often considered a more rigorous criterion for determining the onset of mass transport limitation in the film. Therefore, this criterion, given by Eq. (28), was applied to determine if there was any mass transfer limitation during the collection of the kinetic data:

$$\frac{\left(-r_{A,obs}\right)\rho_b nR}{k_c C_A} < 0.15 \tag{28}$$

The value of the left side of Eq. (28) was 5.7×10^{-3}, which is far less than 0.15. Hence, it can be concluded that there was no mass transport limitation in the film.

The experimental parameters and conditions used in collecting the kinetic data are shown in Tables 2 and 3. Table 3 also contains the variation of crude ethanol conversion with space time at reaction temperatures 673, 763 and 863 K. The plot of crude ethanol conversion, X_E, against space time is shown in Fig.1.

4.2. Experiments

In order to ensure plug flow conditions (i.e. zero radial velocity and temperature profile), absence of back-mixing, and absence of channelling, the criteria reported by Rase [66] and Froment and Bischoff [57] were utilised. These criteria are: $\left(z_T/d_P\right)\geq 50$ and $\left(d/d_P\right)\geq 10$. In this study, $\left(z_T/d_P\right)$ and $\left(d/d_P\right)$ were calculated to be 88.33 and 13.33 respectively, and, hence the conditions for plug flow were met. Internal mass transfer resistance was considered to be negligible and isothermal reaction conditions were assumed inside the porous bed. The pressure drop inside the bed was assumed to be negligible.

4.3. Discussion

Figure 1 shows the experimental results for the variation of fractional conversion, X_E, of crude ethanol with ratio of weight of catalyst to flow rate of crude ethanol W/N_{E0} at reaction temperatures of 673, 763 and 863 K. These results show that the fractional conversion of crude ethanol increased with an increase in W/N_{E0}.

The proposed empirical, irreversible power rate law models given by Eqs. (8)-(10) were fitted to the experimental data using the non-linear least squares method

Table 2. Experimental Kinetic Data.

T(K)	N_E (mol/h)	N_W (mol/h)	N_C (mol/h)	N_H (mol/h)	Experimental rate (g mol crude ethanol/g cat. h)
673	0.0691	0.2509	0.0750	0.2094	$5.37\times10^{-2} \pm 0.0003$
	0.0639	0.2354	0.0862	0.2408	$4.05\times10^{-2} \pm 0.0005$
	0.0612	0.2271	0.0922	0.2576	$2.95\times10^{-2} \pm 0.0004$
	0.0559	0.2113	0.1037	0.2897	$9.85\times10^{-3} \pm 0.0001$
763	0.0529	0.2023	0.1102	0.3079	$1.49\times10^{-2} \pm 0.0003$
	0.0576	0.2165	0.1000	0.2792	$7.09\times10^{-2} \pm 0.0008$
	0.0518	0.1992	0.1125	0.3142	$3.94\times10^{-2} \pm 0.0006$
	0.0478	0.1872	0.1212	0.3386	$2.79\times10^{-2} \pm 0.0008$
	0.0429	0.1724	0.1320	0.3686	$1.55\times10^{-2} \pm 0.0002$
	0.0380	0.1579	0.1425	0.3979	$1.01\times10^{-2} \pm 0.0001$
863	0.0495	0.1924	0.1175	0.3281	$1.13\times10^{-1} \pm 0.0005$
	0.0425	0.1713	0.1327	0.3707	$5.64\times10^{-2} \pm 0.0007$
	0.0369	0.1545	0.1450	0.4049	$3.76\times10^{-2} \pm 0.0009$
	0.0288	0.1304	0.1625	0.4538	$1.88\times10^{-2} + 0.0007$
	0.0242	0.1166	0.1725	0.4817	$1.13\times10^{-2} \pm 0.0004$

Table 3. Reaction Conditions and Parameters used in Collecting Kinetic Data: N_{Eo} = 0.1037 Mol Crude Ethanol/h [46].

T (K)	W (g)	W/N_{Eo} (kg cat. h/kmol crude ethanol	Conversion, X_E
673	0.1	0.9645	0.33 ± 0.0013
763			0.44 ± 0.0052
863			0.52 ± 0.0011
673	0.2	1.9290	0.38 ± 0.0034
763			0.50 ± 0.0004
863			0.59 ± 0.0064
673	0.3	2.8935	0.41 ± 0.0034
763			0.54 ± 0.0076
863			0.64 ± 0.0039
673	0.6	5.7870	0.46 ± 0.0044
763			0.59 ± 0.0037
863			0.72 ± 0.0064
673	1.0	9.6451	0.49 ± 0.0012
763			0.63 ± 0.0047
863			0.77 ± 0.0047

of analysis and none of the models correlated the experimental data well within the range of temperatures investigated in this study. Hence, the power rate law cannot be used to describe the kinetics of steam reforming of crude ethanol on Ni/Al_2O_3 catalyst in the temperature range of 673-863 K.

The constants for calculating equilibrium constant K_{SR} are presented in Table 4.

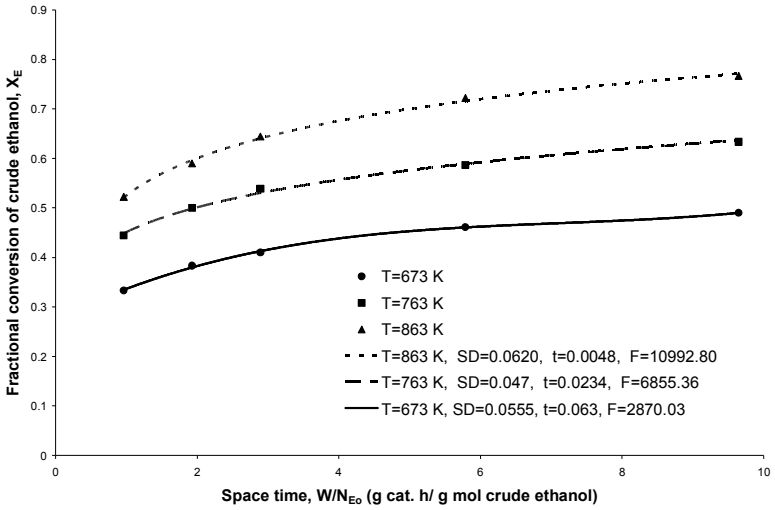

Fig. 1. Comparison of Experimental and Predicted Fractional Conversion of Crude Ethanol against Space Time at Different Temperature Levels.

Table 4. Constants for Calculating Equilibrium Constant, K_{SR} [67].

Component	*a*	*b*	*c*	*d*	$\Delta H^0_{f,298K}$ (J/mol)	$\Delta G^0_{f,298K}$ (J/mol)
C_2H_5OH	3.518	2.00×10^{-2}	-6.002×10^{-6}	0	-235,100	-168,490
H_2O	3.470	1.45×10^{-3}	0	1.21×10^{4}	-241,818	-228,572
CO_2	5.457	1.045×10^{-3}	0	-1.157×10^{5}	-393,509	-394,359
H_2	3.249	4.22×10^{-4}	0	8.30×10^{3}	0	0

where $\Delta = 6.06\times H_2 + 2.17\times CO_2 - C_2H_5OH - 2.99\times H_2O$. Hence, $\Delta a = 17.64$, $\Delta b = -0.0195$, $\Delta c = 6.002E-06$, $\Delta d = -237601$, $\Delta H^0_0 = 104{,}221.29$ J/mol and $\Delta G^0_0 = -3838.75$ J/mol.

Selection of the best model was based on the positiveness of the rate and equilibrium constants, the goodness of fit as determined by the values of the objective function, the decrease of the specific reaction rate constants, k_i, k_i', and increase of thermodynamic equilibrium constants, K_i, with increase in temperature respectively, thermodynamic scrutiny and statistical tests. Particular difficulties associated with the optimisation problem arise because non-linear systems can have more than one optimum. The optimisation method of Nelder and Mead is capable of finding one or more of the optimum points depending on the initial guesses and step sizes used. It was observed that at initial guesses and step sizes of 0.5, 1.0 and 5, there was no effect of change in step size on the values of the optima.

Amongst the rival models, the best fit of the experimental conversion/rate against W/F_{Mo} data with positive rate and equilibrium constants was obtained for surface reaction between chemisorbed CH_3O and O as the rate-determining step during steam reforming of crude ethanol, with oxygen and hydrogen being adsorbed as a monomolecular species on the catalyst surface, that is:

$$(-r'_M)=\frac{\dfrac{k_{S2}\left(K_C K_{MH} K_H\right)^{1/2} K_{SR}}{K_{S2}} C_T^4\left(\dfrac{C_E C_W^3}{C_C C_{H_2}^{9/2}}-\dfrac{1}{K_{SR}} C_C C_{H_2}^{3/2}\right)}{\left[1+K_E C_E+\dfrac{K_M K_E K_{S3}\left(K_{S1} K_W\right)^{2/3}}{\left(K_C K_{MH} K_H\right)^{1/2}}\dfrac{C_E C_W^2}{C_C C_{H_2}^{7/2}}+\dfrac{\left(K_C K_{MH} K_H\right)^{1/2}}{K_{S3}\left(K_{S1} K_W\right)^{2/3}}\right.} \times \frac{C_C C_{H_2}^{7/2}}{C_W^2}$$

$$\left.+K_W^{1/3} C_W+\left(K_{S1} K_W\right)^{1/3}\frac{C_W}{C_{H_2}}+K_C^{1/2} C_C+\left(K_{MH} K_H\right)^{1/6} C_{H_2}^{1/2}+K_H^{1/3} C_{H_2}\right]^4 \qquad (29)$$

The predicted results are shown in Table 5, with the objective function values. From the estimated kinetic constants, the forward and backward activation energies, and the enthalpy of adsorption with corresponding pre-exponential/frequency factor were evaluated using the least-squares technique via the application of the Arrhenius law and plots, and Van't Hoff law and plot respectively. The adsorption entropy change, ΔS_{ads}, for the process was computed using Eq. (22). The temperature dependencies of the surface reaction rate coefficients, k_{S2}, k'_{S2} and of the adsorption equilibrium constants, K_{SR} are depicted in Figures 2 and 3 respectively. The corresponding forward and backward activation energies, E_f and E_b, enthalpies of adsorption, ΔH_{ads}, and adsorption entropy change, ΔS_{ads}, were computed and their calculated values are shown in Table 6, together with respective frequency factors. From this table, it can be deduced that the condition spelt out in Eq. (27) is satisfied, that is, for steam reforming of crude ethanol on Ni/Al_2O_3 catalyst, -427.64<-176.83<10, implying that model 5, expressed in Eq. (29) satisfies thermodynamic scrutiny.

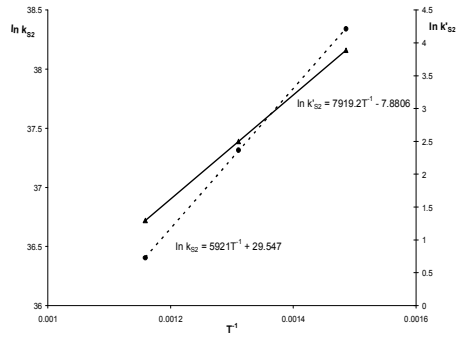

Fig. 2. Variation of Forward and Backward Surface Reaction Rate Constants with Temperature during Steam Reforming of Concentrated Crude Ethanol on Ni/Al_2O_3 Catalyst.

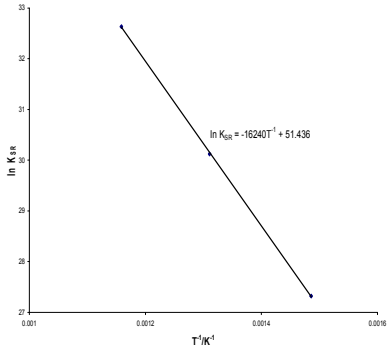

Fig. 3. In K_{SR} against T^{-1} for Steam Reforming of Concentrated Crude Ethanol on Ni/Al_2O_3 Catalyst.

Table 5. Estimated Kinetic Parameters for Steam Reforming of Crude Ethanol with Hydrogen and Oxygen Being Adsorbed as a Monomolecular Species on Ni/Al_2O_3 Catalyst.

Parameter	Temperature		
	673 K	**763 K**	**863 K**
k_{S2}	4.5838×10^{16}	1.6043×10^{16}	6.4599×10^{15}
k'_{S2}	48.7330	12.1627	3.6536
K_{S2}	9.41×10^{14}	1.32×10^{15}	1.77×10^{15}
K_C	1.7834×10^{-5}	7.9683×10^{-4}	2.1437×10^{-2}
K_{MH}	0.8119	103.8125	6945.87
K_H	2.1719×10^{-3}	0.1472	5.6825
K_{SR}	7.3220×10^{11}	1.2068×10^{13}	1.4887×10^{14}
K_E	0.1365	1.9157	18.8928
K_M	0.1881	7.0086	161.1188
K_{S3}	1.25×10^{-4}	4.09×10^{-4}	1.25×10^{-3}
K_{S1}	6.3279×10^{-4}	4.1890×10^{-4}	1.5844
K_W	0.0121	0.4843	11.8426
C_T	0.1616	0.3470	0.6042
Objective function	8.1103×10^{-6}	5.4372×10^{-6}	3.7759×10^{-7}

Table 6. Calculated Values of Energies and Frequency Factors for the Preferred Model for Steam Reforming of Crude Ethanol on Ni/Al_2O_3 Catalyst.

Model	E_f (J/mol)	Frequency factor	E_b (J/mol)	Frequency factor	ΔH_{ads} (J/mol)	Frequency factor	ΔS_{ads} (J/mol K)
5	-4.98×10^{4}	6.8×10^{12}	-6.58×10^{4}	3.78×10^{-4}	1.35×10^{5}	2.18×10^{22}	427.64

The excellent agreement between the model predictions and the experimentally measured conversions is shown in Fig. 1, with their corresponding standard deviation (SD), S_d, calculated F and t values. The kinetic model 5 has the highest F values amongst rival models. However, the model with the highest F value is the most preferred. In order to ascertain the validity range of the kinetic expression as proposed by this model, a rigorous error analysis was incorporated by carrying out a residual analysis. If the model is adequate, the residuals should be structureless [68, 69]. Figure 4 depicts plots of residuals versus predicted conversion of crude ethanol. It is seen that there is no obvious patterns. Therefore, model 5 is preferred to other rival models since its estimated kinetic parameters have satisfied the physicochemical constraints. Moreover, the kinetic parameters were positive, statistically significantly different from zero, and they satisfied the thermodynamic conditions of model adequacy. The preferred model is given by Eq. (29).

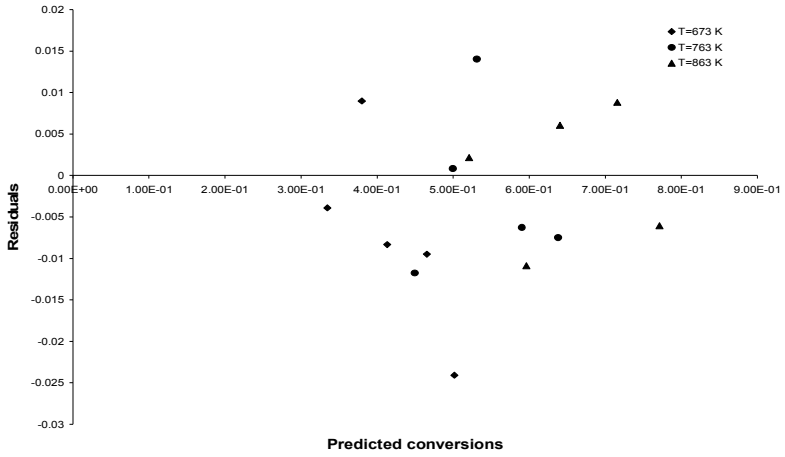

Fig. 4. Residuals against Predicted Ethanol Conversions at Different Temperature Levels.

5. Conclusion

The rate-determining step for the steam reforming of concentrated crude ethanol on Ni/Al_2O_3 catalyst, which can be used for sizing the reformer and optimization studies, was found to be surface reaction between chemisorbed CH_3O and O when hydrogen and oxygen are adsorbed as monomolecular species on the catalyst surface.

References

1. Torkmahalleh, M.A.; Lin, L.; Holsen, T.M.; Rasmussen, D.H.; and Hopke, P.K. (2012). The impact of deliquescence and pH on Cr speciation in ambient PM samples. *Aerosol Science and Technology*, 46(6), 690-696.
2. Torkmahalleh, M.A.; Lin, L.; Holsen, T.M.; Rasmussen, D.H.; and Hopke, P. K. (2013). Cr speciation changes in the presence of ozone and reactive oxygen species at low relative humidity. *Atmospheric Environment*, 71, 92-94.
3. Torkmahalleh, M.A.; Zhao, Y.; Hopke, P.K.; Rossner, A.; and Ferro, A.R. (2013). Additive impacts on particle emissions from heating low emitting cooking oils. *Atmospheric Environment*, 74, 194-198.
4. Cortright, R.D.; Davda, R.R.; and Dumesic, J.A. (2002). Hydrogen from catalytic reforming of biomass-derived hydrocarbon in liquid water. *Letters to Nature*, 418, 964-967.
5. Haga, F.; Nakajima, T.; Yamashita, K.; and Mishima, S. (1998). Effect of crystallite size on the catalysis of Alumina-supported cobalt catalyst for steam reforming of ethanol. *Reaction Kinetic & Catalysis Letter*, 63(2), 253-259.
6. Creveling, H.F. (1992). Proton Exchange Membrane (PEM) fuel cell system R & D for transportation applications. *Proceedings of Annual Automotive Technology Development Contractors' Coordination Meeting, Society of Automotive Engineers*, 485-492.

7. Whitaker, F.L. (1994). The Phosphoric Acid PC 25^{TM} fuel cell power plant and beyond. *AIAA 29th Intersociety of Energy Conversion & Engineering Conference*, Monterey, CA., 1258-1259.
8. Klouz, V.; Fierro, V.; Denton, P.; Katz, H.; Lisse, J.P.; Bouvot-mauduit, S.; and Mirodatos, C. (2002). Ethanol reforming for hydrogen production in a hybrid electric vehicle: process optimization. *Journal of Power Sources*, 105(1), 26-34.
9. Gary, J.H.; and Handwerk, G.E. (1994). *Petroleum refining technology and economics*. 3rd Edition, Marcel Dekker, Inc.
10. Simanzhenkov, V.; and Idem, R.O. (2003). *Crude oil chemistry*. Marcel Dekker, New York.
11. Garcia, L.; French, R.; Czernik, S.; and Chornet, E. (2000). Catalytic steam reforming of bio-oils for the production of Hydrogen: effects of catalyst composition. *Applied Catalysis*, 201, 225-239.
12. Momirlan, M.; and Veziroglu (2005). The properties of hydrogen as fuel tomorrow in sustainable energy system for a cleaner planet. *International Journal of Hydrogen Energy*, 30(7), 795-802.
13. Athanasio, N.F.; and Verykios, X.E. (2004). Reaction network of steam reforming of ethanol over Ni-based catalysts. *Journal of Catalysis*, 225, 439-452.
14. Cavallaro, S.; and Freni, S. (1996). Ethanol steam reforming in a molten carbonate fuel cell: A preliminary kinetic investigation. *International Journal of Hydrogen Energy*, 21(6), 465-469.
15. Athanasios, N.F.; and Kondaridesm, D.I. (2002). Production of hydrogen for fuel cells by reformation of biomass-derived ethanol, *Catalysis Today*, 75, 145-155.
16. Akande, A.J. (2005). *Production of hydrogen by reforming of crude ethanol*. M.Sc. Thesis, Department of Chemical Engineering, University of Saskatchewan, Saskatoon, Saskatchewan, Canada.
17. Garcia, E.Y.; and Laborde, M.A. (1991). Hydrogen production by the steam reforming of ethanol: Thermodynamic Analysis. *International Journal of Hydrogen Energy*, 16(5), 307-312.
18. Freni, S.; Maggio, G.; and Cavallaro, S. (1996). Ethanol steam reforming in a molten carbonate fuel cell: A thermodynamic approach. *Journal of Power Sources*, 62(1), 67-73.
19. Theophilos, I. (2001). Thermodynamic analysis of ethanol processors for fuel cell applications. *Journal of Power Sources*, 92(-2), 17-25.
20. Vasudeva, K.; Mitra, N.; Umasankar, P.; and Dhingra, S.C. (1996). Steam reforming of ethanol for hydrogen production: Thermodynamic Analysis. *International Journal of Hydrogen Energy*, 21(1), 13-18.
21. Jordi, L.; Homs, N.; Sales, J.; and Ramirez de la Piscina, P. (2002). Efficient production of hydrogen over supported cobalt catalysts for ethanol reforming. *Journal of Catalysis*, 209(2), 306-317.
22. Leclerc, S.; Mann, R.F.; and Peppley, B.A. (1998). Evaluation of the catalytic ethanol-steam reforming process as a source of hydrogen-rich gas for fuel cells. *Prepared for the CANMET Energy Technology Centre (CETC)*.

23. Galvita, A.A.; Semin, G.L.; Belyaev, V.D.; Semikolenov, V.A.; Tsiakaras, P.; and Sobyanin, V.A. (2001). Synthesis gas production by steam reforming of ethanol. *Applied Catalysis A: General*, 220(1-2), 123-127.
24. Das, N. (2003). *Low temperature steam reforming of ethanol*. Masters Thesis, Department of Chemical Engineering, University of Saskatchewan.
25. Marino, F.; Cerrella, E.; Duhalde, S.; Jobbagy M.; and Laborde, M. (1998). Hydrogen from steam reforming of ethanol: Characterization and performance of copper-nickel supported catalysts. *International Journal of Hydrogen Energy*, 23(12), 1095-1101.
26. Luengo, C.A.; Ciampi, G.; Cencig, M.O.; Steckelberg, C.; and Larbode, M. A. (1992). A novel catalyst system for ethanol gasification. *International Journal of Hydrogen Energy*, 17(9), 667-681.
27. Velu, S.; Satoh, N.; and Gopinath, S.C. (2002). Oxidative reforming of bio-ethanol over CuNiZnAl, mixed oxides catalysts for hydrogen production. *Catalysis Letters*, 82(1-2), 145-151.
28. 28. Jordi, L.; and Ramirez, P. (2001). Direct production of hydrogen from ethanol aqueous solutions over oxide catalysts. *The Royal Society of Chemistry Chemical Communication*, 641-642.
29. Aupretre, F.; Descorme, C.; and Duprez, D. (2002). Bio-ethanol catalytic steam reforming over supported metal catalyst. *Catalysis Communication*, 3(6), 263-267.
30. Breen, J.P.; Burch, R.; and Coleman, H.M. (2002). Metal-catalyzed steam reforming of ethanol in the production of hydrogen for fuel cell applications. *Applied Catalysis B: Environmental*, 39(1), 65-74.
31. Cavallaro, S.; Chiodo, V.; Freni, S.; Mondello, N.; and Frusteri, F. (2003). Performance of Rh/Al_2O_3catalyst in the steam reforming of ethanol: H_2 production for MCFC. *Applied Catalysis A: General*, 249(1), 119-128.
32. Freni, S. (2001). Rh based catalysts for indirect internal reforming ethanol applications in molten carbonate fuel cells. *Journal of Power Sources*, 94(1), 14-19.
33. Freni, S.; Cavallaro, S.; Mondello, N.; Spadaro, L.; and F. Frusteri, F. (2002). Steam reforming of ethanol on Ni/MgO catalyst: H_2 production for MCFC. *Journal of Power Sources*, 108(1-2), 53-57.
34. Jose, C.; Marino, F.; Laborde, M.; and Amadeo, N. (2004). Bio-ethanol steam reforming on Ni/Al_2O_3 catalyst. *Chemical Engineering Journal*, 98(1-2), 61-68.
35. Mavrikakis, M.; and Barteau, M.A. (1998). Oxygenated reaction pathways on transition metal surfaces. *Journal of Molecular Catalysis*, 131(1-3), 135-147.
36. Therdthianwong, A.; Sakulkoakiet, T.; and Therdthianwong, S. (2001). Hydrogen production by catalytic ethanol steam reforming. *Science Asia*, 27, 193-198.
37. Diagne, C.; Idris, H.; and Kiennemann, A. (2002). Hydrogen production by ethanol reforming over Rh/CeO2-ZrO2 catalysts. *Catalysis Communication*, 3(12), 565-571.

38. Sheng, P.Y.; Yee, A.; Bowmaker, G.A.; and Idris, H. (2002). H_2 production from ethanol over Rh-Pt/CeO2 catalysts: the role of Rh for the efficient dissociation of the carbon-carbon bond. *Journal of Catalysis*, 208(2), 393-403.
39. Fatsikostas, N.A.; and Verykios, X.E. (2004). Reaction network for steam reforming of ethanol over Ni-based catalysts. *Journal of Catalysis*, 225(2), 439-452.
40. Marino, F.; Boveri, M.; Baronetti, G.; and Laborde, M. (2004). Hydrogen production via catalytic gasification of ethanol: A mechanism proposal over copper-nickel catalysts. *International Journal of Hydrogen Energy*, 29(1), 67-71.
41. Kugai, J.; Velu, S.; and Song, C. (2005). Low temperature reforming of ethanol over CeO_2-supported Ni-Rh bimetallic catalysts for hydrogen production. *Catalysis Letters*, 101(3-4), 255-264.
42. Sun, J.; Qiu, X.; Wu, F.; and Zhu, W. (2005). H_2 from steam reforming of ethanol at low temperature over Ni/Y_2O_3, Ni/La_2O_3 and Ni/Al_2O_3 catalysts for fuel-cell application. *International Journal of Hydrogen Energy*, 30(4), 437-445.
43. Akande, A.; Aboudheir, A.; Idem, R; and Dalai, A. (2006). Kinetic modeling of hydrogen production by the catalytic reforming of crude ethanol over a Co-precipitated $Ni-Al_2O_3$ catalyst in a packed bed tubular reactor. *International Journal of Hydrogen Energy*, 31(12), 1707-1715.
44. Vaidya, P.D.; and Rodrigues, A.E. (2006). Kinetics of steam reforming of ethanol over a Ru/Al_2O_3 catalyst. *Industrial & Engineering Chemistry Research*, 45(19), 6614-6621.
45. Akande, A.; Idem, R.; and Dalai, A. (2005). Synthesis, characterization and performance evaluation of Ni/Al_2O_3 catalysts for reforming of crude ethanol for hydrogen production. *Applied Catalysis A: General*, 287(2), 159-175.
46. Akpan, E.; Akande, A.; Aboudheir, A.; Ibrahim, H.; and Idem, R. (2007). Experimental, kinetic and 2-D reactor modeling for simulation of the production of hydrogen by the catalytic reforming of concentrated crude ethanol (CRCCE) over a Ni-based commercial catalyst in a packed-bed tubular reactor. *Chemical Engineering Science*, 62(12), 3112-3126.
47. Lee, J.K., Ko, J.B. and Kim, D.H. (2004). Methanol steam reforming over $Cu/ZnO/Al_2O_3$ catalyst: kinetics and effectiveness factor. *Applied Catalysis A: General*, 278(1), 25-35.
48. Richardson, J.T. (1989). *Principles of catalyst development*. Plenum Press, New York.
49. Agarwal, V.; Sanjay, P.; and Pant, K.K. (2005). H_2 production by steam reforming of methanol over $Cu/ZnO/Al_2O_3$ catalysts: transient deactivation kinetics modelling. *Applied Catalysis A: General*, 275(1-2), 155-164.
50. Yang, W.Y.; Cao, W.; Chung, T.; and Morris, J. (2005). *Applied numerical methods using MATLAB*. A John Wiley & Sons Inc., Publication (Wiley Interscience), 325-328.
51. Olafadehan, O.A.; and Susu, A.A. (2004). Computerized solution of the dynamic sorption process for a ternary system in a heterophase medium. *Theoretical Foundations of Chemical Engineering*, 38(2), 140-151.
52. Olafadehan, O.A.; and Susu, A.A. (2005). Numerical solution of binary liquid-phase adsorption on porocel clay using linear, Freundlich and Langmuir Isotherms. *Adsorption Science & Technology*, 23(3), 195-214.

53. Olafadehan, O.A.; and Okinedo, E.U. (2009). Mechanistic kinetic models for hydrogenolysis of benzothiophene on Co-Mo/γ-Al_2O_3 catalysts. *Petroleum Science & Technology*, 27(3), 239-262.
54. Olafadehan, O.A.; and Oghenekaro, S.O. (2008). Kinetic models for hydrogenolysis of thiophene on Co-Mo/γ-Al_2O_3 catalysts. *Petroleum Science & Technology*, 26(3), 278-297.
55. Olafadehan, O.A., Susu, A.A.; and Jaiyeola, A. (2008). Mechanistic kinetic models for n-heptane reforming on platinum/alumina catalysts. *Petroleum Science & Technology*, 26(12), 1459-1480.
56. Press, W.H.; Flannery, B.P.; Teukolsky, S.A.; and Vetterling, W.T. (1992). *Numerical recipes.* Cambridge University Press.
57. Froment, G.F.; and Bischoff, K.B. (1990). *Chemical reactor analysis and design.* John Wiley and Sons, Inc.
58. Boudart, M.; Mears, D.E.; and Vannice, M.A. (1967). *Industry Chimique Belge*, 32, 281-301.
59. Vannice, M.A.; Hyun, S.H.; Kalpakci, B.; and Liauh, W.C. (1979). Entropies of adsorption in heterogeneous catalytic reactions. *Journal of Catalysis*, 56(3), 358-362.
60. Levenspiel, O. (1999). *Chemical reaction engineering*. 3rd ed., Wiley, New York.
61. Fogler, H.S. (1999). *Elements of chemical reaction engineering*. 3rd ed., Prentice-Hall, Englewood Cliffs, NJ.
62. Perry, R.H.; and Green, D.W. (1997). *Perry's Chemical Engineers' Handbook*. 7th ed., McGraw-Hill, New York.
63. Walas, S.M. (1990). Chemical process equipment - selection and design, Butterworth-Heinemann, Newton, MA.
64. Geankoplis, C.J. (2003). *Transport processes and separation process principles*. 4th ed., Wiley, New York.
65. Mears, D.E. (1971). Tests for transport limitations in experimental catalytic reactors. *Industrial & Engineering Chemistry Process Design and Development*, 10(4), 541-547.
65. Rase, H.F. (1987). *Chemical reactor design for process plants*. Wiley, N.Y.
66. Smith, J.M.; Vanness, H.C.; and Abbott, M.M. (1996). *Introduction to chemical engineering thermodynamics*. 5th Edition, McGraw-Hill.
67. Montgomery, D.C. (1991). *Design and analysis of experiments.* John Wiley and Sons, New York.
68. Olafadehan, O.A.; Taiwo, O.P; and Aribike, D.S. (2009). Kinetics and mechanisms of steam reforming of methanol on Cu/ZnO/Al_2O_3 catalyst. *Journal of Engineering Research*, 14(2), 47-62.